Journal of Nuclear Medicine, published on July 3, 2020 as doi:10.2967/jnumed.120.243394

TAG-72 targeted α-radionuclide therapy of ovarian cancer using actinium-225 labeled DOTAylated-huCC49 antibody

Megan Minnix [1,2], Lin Li [1], Paul J. Yazaki [1], Aaron D. Miller[1], Junie Chea [3], Erasmus Poku [3], An Liu[4], Jeffrey Y.C. Wong[4], Russell C. Rockne[5], David Colcher [1] and John E. Shively [1,*]

[1]Department of Molecular Imaging and Therapy, Beckman Research Institute, City of Hope, Duarte, CA, 91010.

[2]Irell and Manella Graduate School of Biological Sciences, Beckman Research Institute, City of Hope, 1500 East Duarte Road, Duarte, CA, 91010.

[3]Radiopharmacy, City of Hope Medical Center, Duarte CA 91010.

[4]Department of Radiation Oncology, City of Hope Medical Center, Duarte CA 91010.

[5]Division of Mathematical Oncology, Beckman Research Institute, City of Hope, Duarte, CA, 91010.

*To whom to address correspondence: John E. Shively, 1500 East Duarte Rd, Duarte, CA 91010, TEL: 626-308-8308, email: jshively@coh.org

running title: ^{225}Ac-DOTA-CC49 ovarian cancer therapy

word count: 4778

author contributions: MM designed, carried out experiments, analyzed data, wrote the first draft; LL, PY, ADM, JC, EP, and RCR contributed valuable materials and data analysis, DC and JES supervised the study.

ABSTRACT

Radioimmunotherapy, an approach using radiolabeled antibodies, has had minimal success in the clinic with several β-emitting radionuclides for the treatment of ovarian cancer. Alternatively, radioimmunotherapy with α-emitters offers the advantage of depositing much higher energy over shorter distances, but were thought to be inappropriate for the treatment of solid tumors where antibody penetration is limited to a few cell diameters around the vascular system. However, the deposition of high energy α-emitters to tumor markers adjacent to a typical leaky tumor vascular system may have large anti-tumor effects at the tumor vascular level, while their reduced penetration in normal tissue would be expected to lower off-target toxicity. **Methods**: To evaluate this concept, DOTAylated-huCC49 was labeled with the α-emitter actinium-225 to target TAG-72 positive xenografts in a murine model of ovarian cancer. **Results**: Actinium-225 labeled DOTAylated-huCC49 radioimmunotherapy significantly reduced tumor growth in a dose dependent manner (1.85, 3.7, and 7.4 kBq), with the 7.4 kBq dose extending survival by more than 3-fold compared to the untreated control. Additionally, a multi-treatment regime (1.85 kBq followed by 5 weekly doses of 0.70 kBq for a total of 5.4 kBq) extended survival almost 3-fold compared to the untreated control group without significant off-target toxicity. Conclusion: These results establish the potential for antibody targeted α-radionuclide therapy for ovarian cancer, which may be generalized to α– radioimmunotherapy in other solid tumors.

Key words: TAG-72, actinium-225, radioimmunotherapy, ovarian cancer

INTRODUCTION

Ovarian cancer, the fifth cause of cancer death among women, has an overall survival rate of about 50% in patients with all stages of ovarian cancer, but only ~17% survival rate in patients diagnosed with later stage diseases. Since only about 15% of patients are identified in the early stages, there is an urgent need for improved therapies (*1*). Across multiple clinical trials the increase in progression free survival is measured in months (*2-4*). Antibody targeted therapies, including radioimmunotherapy and antibody drug conjugates, offer promise in that they target a cytotoxic agent directly to the tumor. Among the tumor-associated antigens identified in ovarian cancer, TAG-72 expressed in 88% of all stages of ovarian cancer, stands out as an excellent candidate for targeted therapy (*5*). TAG-72 is a mucin-like molecule that arises from aberrantly glycosylated mucins in cancer (*6*). Although TAG-72 is expressed in normal endometrial tissues during the secretory phase, it is over-expressed in a multitude of carcinomas, including ovarian cancer (*7,8*). The monoclonal antibody CC49 was developed for its advantages over the first generation B72.3 antibody (*9*). Although anti-TAG-72 antibodies exhibit excellent tumor targeting in both preclinical models and in the clinic (*10*), they have no therapeutic effects on their own, requiring conjugation to therapeutic agents.

β-Emitting radionuclides have been investigated for radioimmunotherapy in solid tumors due to their high tissue penetration (*11*). In the case of TAG-72 positive solid tumors, three β-emitter radionuclides, Iodine-131 (^{131}I), Yttrium-90 (^{90}Y), and Lutetium-177 (^{177}Lu), on anti-TAG-72 antibodies have been tested for their anti-tumor effects in clinical studies(*12-14*). Unfortunately, radioimmunotherapy clinical trials based on the anti-TAG-72 antibody have never made it past Phase 2 for the treatment of colon cancer and ovarian cancer, due to the lack of a significant clinical response rate and/or the presence of bone marrow toxicity. In general, radioimmunotherapy trials utilizing β-emitters have been shown to exhibit a dose limiting toxicity to the bone marrow due to the high penetrative power of their emissions while the antibody is in circulation (*15*). Recently, radioimmunotherapy using α-emitting radionuclides has been explored due to their higher linear energy transfer and lower penetrative distance (47-85 μm) in tissue

(*16*). Based on their low penetrative power, α-emitting radionuclides in radioimmunotherapy were mainly investigated in the treatment of non-solid cancers such as leukemia and multiple myeloma (*17,18*). Recently the use of α-emitters for the treatment of solid tumors has begun to show promise (*19,20*). Among the newly available α-emitters, actinium-225 (^{225}Ac) stands out due to its long half-life (10 days) and the release of 4 α-particles in its decay scheme (*21*). Examples of preclinical studies with ^{225}Ac-antibody conjugates include treatment of ovarian cancer xenografts (*22*), colon tumor xenografts (*23*), neuroblastoma xenografts (*24*), and breast cancer metastases (*25*). The expression of tumor antigens in close proximity to the tumor vascular system, along with the deposition of higher energies, may make α-radionuclide based radioimmunotherapy more generally effective than other targeted therapies. To test this concept in an OVCAR3 murine model of ovarian cancer, DOTAylated-huCC49 antibody was radiolabeled with the α-emitter ^{225}Ac, and single vs multi-treatment strategies were compared.

MATERIALS AND METHODS

Antibodies, Reagents and Cell Lines. Murine CC49 mAb (muCC49) clone was from ATCC (Manassas, VA) and purified by protein A chromatography. Daratumumab (anti-CD38; Janssen Biotech Inc., Titusville, NJ) was used as an untargeted antibody control. OVCAR3 was from ATCC; DOTA-N-hydroxysuccinimide ester from Macrocyclics, Inc. (Plano, TX); Copper-64 from Washington University (St Louis, MO), Iodine-124 from 3D Imaging (Maumelle, AR), Indium-111 from Curium US LLC (Maryland Heights, MO) and ^{225}Ac from the Department of Energy, Oakridge National Laboratory (Oakridge, TN).

Humanization of Anti-TAG-72 muCC49 Antibody. See Supplemental Material.

Animal Studies. Animal studies were performed in female NOD SCID mice (Jackson Laboratory) in accordance with IACUC protocols 14043 and 91037 approved by the City of Hope Institutional Animal Care and Use Committee, in accordance with the NIH Office of Laboratory Animal Welfare guidelines. OVCAR3 cells were injected s.c. (1.5 x 10^6 cells per mouse) and tumor size measured by calipers $0.5(LxW^2)$. Mice were euthanized once tumors reached 1500mm^3. Whole body toxicity was measured by weight loss with >20% weight loss considered an endpoint.

Radiolabeling Studies. DOTAylated-mAbs (30 molar excess of DOTA-N-hydroxysuccinimide ester) were radiolabeled with ^{64}Cu at a ratio of 0.37:1 MBq/µg,^{124}I at a ratio of 0.37:1 MBq/µg, ^{111}In at a ratio of 0.37:1 MBq/µg or ^{225}Ac at a ratio of 1.85:1 kBq/µg, and purified by SEC on a 10/30 GL column (GE Biosciences). Radiolabel efficiencies were 89-100% by ITLC. The average number of chelates per antibody were determined by Q-TOF mass spectrometry. Immunoreactivity was determined by incubation with a 20-fold excess of bovine submaxillary mucin to the radiolabeled antibody followed by SEC chromatography.

PET Imaging, Biodistribution Studies and Pharmacokinetics. Tumor-bearing mice were injected IV with radiolabeled mAbs (3.7 kBq/mouse for ^{64}Cu; 0.37 kBq/mouse for ^{124}I or ^{111}In), following an IVIg i.p. injection of 1 mg/mL per mouse 2 hours prior, and

imaged at various times on a Siemens Inveon PET/CT, Knoxville, TN. Images were reconstructed as previously described (*26*). For ^{124}I studies, mice were given potassium iodide (SSKI) 24-48 hours prior to injections (*27*).

Therapy Studies. Mice (tumor size 50-100 mm^3) were treated with saline, or untargeted control mAb (^{225}Ac-DOTAylated-Dara), or targeted mAb (^{225}Ac-DOTAylated-huCC49), given IV, following IVIg. For the multi-treatment study, mice were injected weekly, for a total of 6 doses. All therapy doses were made up to 30 µg mAb by the addition of unlabeled mAb.

Statistical Analysis. One-way ANOVA (Tukey's multiple comparison test) were used to compare the tumor growth curves of each treatment group to the untreated saline control group. A log-rank Mantel-Cox test was used for the survival curves. Survival was defined as the time (t) in which the tumor had reached a volume of 1500 mm^3 (y). All statistical analyses were performed in Prism 7.02 (GraphPad Software).

Absorbed Dose calculations. See supplemental information for these calculations.

RESULTS

TAG-72 Expression in OVCAR3 Tumors. The OVCAR3 tumors had strong staining for TAG-72 expression with huCC49 and were negative for CD38 with anti-CD38 (Dara) (Supplemental Figure S1).

Radiolabeling and Pharmacokinetics of DOTAylated-huCC49. Conjugation of huCC49 with DOTA-N-hydroxysuccinimide gave a product with an average of 6 chelates per antibody, >90% labeling with ^{225}Ac, and >85% immunoreactivity (Supplemental Figure S2). Blood clearance of muCC49 and huCC49 showed similar half-lives of 17.7 hours and 16.7 hours, respectively (Supplementary Figure S3). PET images of ^{64}Cu-DOTAylated-huCC49 show that huCC49 antibody targeted OVCAR3 tumors (Figure 1A), reaching 26% injected dose/gram (ID/g) at 46 hours post injection (Figure 1B).

Single Treatment Radioimmunotherapy Study. Single treatments of OVCAR3 xenografts with 1.85 kBq, 3.7 kBq, or 7.4 kBq of ^{225}Ac-DOTAylated-huCC49 led to a dose dependent reduction in tumor growth (Figure 2A). While the 1.85 kBq dose of ^{225}Ac-DOTAylated-huCC49 did not show a significant difference, there was a significant difference in the 3.7 and 7.4 kBq doses compared to the control. The untargeted ^{225}Ac-DOTAylated-Dara control dose of 7.4 kBq was equivalent to the targeted dose of 3.7 kBq. The tumor response seen with the 7.4 kBq untargeted control dose was likely due to enhanced permeability and retention (EPR) of antibodies. The EPR effect is the favored accumulation of >40kDa molecules in tumors over normal tissues (*28*).

There was a significant dose dependent increase in survival (Figure 2B). In this analysis mean survival was extended from 32.3 days in the vehicle control to 54.6 days in the 1.85 kBq targeted dose, while the 3.7 kBq targeted dose extended survival to 81.6 days and the 7.4 kBq targeted dose extended survival to 103 days (Table 1). Thus, the mean survival time of the 7.4 kBq targeted treatment group was >3X the mean survival time compared to the control group, with 3 out of 6 mice maintaining reduced tumor growth past day 100 (Supplementary Figure S4). The 7.4 kBq untargeted

antibody control group showed a similar survival advantage as the 3.7 kBq ^{225}Ac-DOTAylated-huCC49 group.

Whole body toxicity was measured as percent weight loss following radioimmunotherapy. Although there was a dose dependent weight loss with the ^{225}Ac-DOTAylated-huCC49 targeted treatment groups, the weights were maintained within the acceptable <20% weight loss (Supplementary Figure S5). Overall, the 7.4 kBq targeted ^{225}Ac-DOTAylated-huCC49 group improved whole body toxicity compared to the 7.4 kBq untargeted control group, likely due to its longer circulation time.

TAG-72 expression was monitored after a single targeted dose of 3.7 kBq ^{225}Ac-DOTAylated-huCC49 at 1, 3, and 5 weeks post the initial 3.4 kBq ^{225}Ac-DOTAylated-huCC49 radioimmunotherapy injection by injection with ^{64}Cu-DOTAylated-huCC49 and terminal biodistribution after 3 days. huCC49 uptake correlated to tumor size, confirming that TAG-72 expression was not reduced by a single treatment of ^{225}Ac-DOTAylated-huCC49 (Figure 3). Since the OVCAR3 xenografts still expressed TAG-72 after a single radioimmunotherapy dose, we explored a multi-treatment regimen.

Multi-treatment Radioimmunotherapy Study. Since the single dose of 1.85 kBq of ^{225}Ac-DOTAylated-huCC49 showed the least amount of whole body toxicity with only a slight increase in survival, we hypothesized that a multi-treatment study with an initial dose of 1.85 kBq followed by subsequent lower doses would have potential benefits over higher single dose regimens. The multi-treatment experiment was designed to maintain the same amount of radioactivity in the tumor over the course of 6 weeks compared to that achieved by a single treatment of 1.85 kBq. Since the 1.85 kBq dose deposited 7.8% of the dose (0.14 kBq) in the tumor (see Figure 1B), subsequent doses were calculated to restore 0.14 kBq in the tumor 7 days later. Thus, we calculated that mice treated with a single 1.85 kBq dose followed by 5 doses of 0.70 kBq of ^{225}Ac-DOTAylated-huCC49 every 7 days would maintain the tumor dose between 0.09-0.14 kBq over each 7 day period (Figure 4A and B). Accounting for radioactive decay, the radioactivity in the tumor (starting at 0.14 kBq) would drop to 0.09 kBq by day 7. A subsequent dose of 0.70 kBq of ^{225}Ac-DOTAylated-huCC49 would boost the amount of radioactivity in the tumor back to 0.14 kBq. This approach allows for the amount of

radioactivity in the tumor to be kept within the initial 1.85 kBq single dose range seen in the first 7 days, but over the course of 6 weeks.

The results of the actual amount of radioactivity delivered to the tumor versus the amount given at the time of injection for each of the 6 doses of ^{225}Ac-DOTAylated-huCC49 was determined by an ^{111}In-DOTAylated-huCC49 tumor uptake study (Figure 4C). Accounting for radioactivity decay between doses, the actual amount of radioactivity in the tumor over time is shown in Figure 4D. The theoretical doses over time (Figure 4B**)** versus actual (Figure 4D**)** closely agree.

The results of the multi-treatment ^{225}Ac-DOTAylated-huCC49 group showed a significant anti-tumor effect compared to the control group, while the untargeted mAb group shows no significant difference, for both the tumor growth (Figure 5A) and survival curves (Figure 5B). The multi-dose ^{225}Ac-DOTAylated-huCC49 group (mean survival of 86.0 days) almost tripled the mean survival compared to both the control group (mean survival of 32.3 days) and the untargeted mAb group (mean survival of 37.6 days; Table 1). In the multi-treatment targeted group, 4/8 mice maintained reduced tumor growth past day 80 and 3/8 mice maintained reduced tumor growth past day 100 (Supplementary Figure S6).

To measure the uptake of targeted vs untargeted mAbs in tumors, the two multi-treatment radioimmunotherapy groups were probed with ^{111}In-labeled mAbs. In the mice that received ^{111}In-labeled untargeted mAb instead of the untargeted radioimmunotherapy, the tumor uptake was 1.51% (Figure 6A). The two mice that received ^{111}In-labeled targeted mAb instead of targeted radioimmunotherapy had a tumor uptake of 5.16% (Figure 6B). Thus, the lack of an anti-tumor response for the multi-treatment untargeted controls can be explained by the uptake of only 1.51% compared to 5.16% for the multi-treatment targeted radioimmunotherapy group. Untargeted mAb uptake correlates to increasing tumor weight (Figure 6A), likely due to the EPR effect. The targeted mAb uptake also correlates with tumor weight (with the exception of a dip after three doses of targeted radioimmunotherapy (Figure 6B), likely due to continued expression of TAG-72. The dip after the third targeted treatment may be due to the selective killing of cells that express the targeted antigen. The resurgence

of TAG-72 expression after the 5th dose suggests that additional targeted radioimmunotherapy could have been performed.

The whole body toxicity of the multi-treatment study indicated no significant difference in weight for the multi-treatment targeted radioimmunotherapy group versus the control group. However, the multi-treatment untargeted radioimmunotherapy group exhibited a significant weight loss compared to the control group (Supplementary Figure S7). In summary, the multi-treatment study demonstrated a significant anti-tumor effect, with no significant whole body toxicity of the multi-treatment targeted radioimmunotherapy compared to multi-treatment untargeted radioimmunotherapy. Since the multi-treatment strategy led to a total dose of 5.4 kBq, a dose falling between two of the single doses administered, we performed an extrapolation of this dose as described in Supplemental Figures S8-11.

Absorbed Radiation Dose in Tumors of Single Treatment vs Multi-treatment Radioimmunoherapy. The absorbed radiation dose in tumors of each of the radioimmunotherapy groups is summarized in Table 1. For the maximum dose, we assumed all of the daughter α-radionuclides remained in the tumor, a likely overestimate. For the minimum dose we assumed that 75% of the daughter α-radionuclides diffused away into the blood stream, a likely under estimate (*29*). The absorbed tumor dose of 10.0max Gy of targeted therapy with a single treatment of 7.4 kBq resulted in the longest survival of 103d compared to 87.9d in which 2.03max Gy of untargeted therapy was delivered to the tumor with a single treatment of 7.4 kBq. Survival was only improved 1.17-fold with targeted over untargeted therapy even with a 5-fold increase in radiation dose to the tumor. Thus, at the highest targeted dose of 7.4 kBq, whole body toxicity has reduced the potential for even better survival that would be predicted by a 5-fold increase in radiation dose. In the case of targeted multi-treatment therapy, a survival of 86d was achieved with a tumor radiation dose of 17.7max Gy compared to 37.6d survival with untargeted multi-treatment tumor radiation dose of 7.74max Gy. There was a 2.29-fold increase in survival with a 2.28-fold increase in radiation dose delivered to the tumor. Thus, a multi-treatment regimen is a promising strategy, in that delivery of the radiation dose over an extended period of time not only reduces whole body toxicity but also leads to a more linear increase in survival.

DISCUSSION

Murine CC49 radiolabeled with ^{225}Ac in a colon cancer model was previously compared to a C_H2-domain deleted CC49 antibody (ΔC_H2 CC49), an antibody fragment predicted to have better tissue penetration and less toxicity than intact IgG (*23*). However, it was found that radioimmunotherapy with Δ C_H2 CC49 had no benefit over intact IgG. In that study, a single dose of 18.5 kBq of ^{225}Ac-muCC49 was found to reduce tumor growth by 18 days, but had unacceptable levels of toxicity. A lower dose of 9.25 kBq was investigated with no evidence of tumor regression. Compared to our results in the ovarian cancer model, these findings suggest that ^{225}Ac-CC49 radioimmunotherapy therapeutic effects may be cancer model specific.

In an α-emitter labeled Muc-1 antibody study in an ovarian cancer model, Song et al. (*30*) showed a single injection of 355 kBq/kg of ^{213}Bi-C595 prolonged survival by 25 days. While encouraging, the short half-life of ^{213}Bi (45 min) has limited its use in the treatment of solid tumor.

A study with ^{225}Ac-DOTA labeled trastuzumab showed high tumor uptake (56-60% ID/g) in a xenograft model of ovarian cancer with a median survival of 52-126 days compared to controls (33-44 days) when treated with 8.14-16.65 kBq of targeted antibody (*22*). This study gave comparable results to our 7.4 kBq targeted dose, but had high toxicity at the higher doses administered, comparable to our 7.4 kBq untargeted dose.

In our study, the treatment of TAG-72 positive OVCAR3 tumors with ^{225}Ac-DOTAylated-huCC49 led to a potent and prolonged anti-tumor effect, suggesting that α-emitter based radioimmunotherapy for solid tumors is feasible. Although we did not determine the physical localization of tumor deposited antibody, it is unlikely that antibody was directed to every tumor cell, since the immunostaining of the tumor xenografts revealed the typical architecture of a solid tumor. Thus, it is likely that the anti-tumor effect was due to other effects.

Although α-emitter based radioimmunotherapy has been shown to effectively treat leukemia and multiple myeloma malignancies (*17,18*), the rationale for α-emitter

based radioimmunotherapy in solid tumors is debatable since it is well known that systemically delivered antibodies remain localized to the interface between the tumor vasculature and the tumor itself (*31*). Since α-particles penetrate no deeper than a few cell diameters, one would predict little effect on tumor cells more than a few cell diameters away from the tumor vasculature. However, if the tumor depends on access to vasculature rich in tumor antigens, a likely situation (*32*), then the deposition of large amounts of energy across the tumor vasculature could be lethal to the entire tumor. Future studies are required to determine if that mechanism is responsible for the anti-tumor effect we observed.

A question that was raised in review concerns the fact that as ^{225}Ac decays, the very short lived daughter radionuclides of ^{221}Fr and ^{217}At produce ^{213}Bi with a half life of 45.62 min that would accumulate over time necessitating removal of accumulated ^{213}Bi prior to its reuse in a multi-treatment strategy (we used the same batch of ^{225}Ac twice, once upon delivery and again after 7d). However, this is of minor concern since the secular amount of ^{213}Bi is the same in both a freshly delivered sample and a 7d old sample of ^{225}Ac (*33*). The amount of ^{213}Bi in the 7d ^{225}Ac was verified by spectral analysis showing the intensity of the 440 keV photon peak of ^{213}Bi was unchanged compared to the 0d sample.

Whole body toxicity remains one of the main drawbacks of radioimmunotherapy. In this respect, whole body toxicity effect was dramatically reduced by performing a multi-treatment regimen. For example, Vallabhajosula et al. (*34*) showed that a fractioned dose regimen of ^{90}Y-DOTA-anti-PSMA antibody was more effective than a single dose and exhibited less toxicity. In our study, we chose a minimally effective single dose of 1.85 kBq that resulted in 0.14 kBq deposited in the tumor, decaying over 7 days, and asked if maintaining this tumor dose over 6 weeks would lead to effective therapy with less whole body toxicity. This was achieved by following the 1.85 kBq initial dose with 5 weekly doses of 0.70 kBq for a total of 5.4 kBq. In fact, the multi-treatment regimen was equally effective as a single 7.4 kBq dose, but with less whole-body toxicity. We conclude that α-emitter based radioimmunotherapy for solid tumors is not only feasible, but can be made less toxic if administered as a multi-dose regimen.

Disclosure: Research reported in this publication was supported by the National Cancer Institute of the National Institutes of Health under award number P30CA033572. No other potential conflict of interest relevant to this article was reported.

Key Points:

1. Is α-radionuclide RIT feasible for the treatment of solid tumors such as ovarian cancer?

2. A dose of 7.4 kBq of ^{225}Ac-DOTAylated-huCC49 resulted in a mean survival of 103 days compared to 32 days for untreated controls with manageable whole body toxicity. A multi-treatment regimen of 1.85 kBq followed by 5 subsequent weekly treatment of 0.70 kBq resulted in a mean survival of 86 days with no whole body toxicity.

3. The clinical implications for this study are that α-radionuclide radioimmunotherapy is feasible for ovarian cancer and that a multi-treatment regimen is effective with negligible whole body toxicity.

REFERENCES

1. Noone AM HN, Krapcho M, Miller D, Brest A, Yu M, Ruhl J, Tatalovich Z, Mariotto A, Lewis DR, Chen HS, Feuer EJ, Cronin KA (eds). SEER Cancer Statistics Review. *National Cancer Institute Bethesda, MD.* 2015.

2. Gonzalez-Martin AJ, Calvo E, Bover I, et al. Randomized phase II trial of carboplatin versus paclitaxel and carboplatin in platinum-sensitive recurrent advanced ovarian carcinoma: a GEICO (Grupo Espanol de Investigacion en Cancer de Ovario) study. *Ann Oncol.* 2005;16:749-755.

3. Pfisterer J, Plante M, Vergote I, et al. Gemcitabine plus carboplatin compared with carboplatin in patients with platinum-sensitive recurrent ovarian cancer: an intergroup trial of the AGO-OVAR, the NCIC CTG, and the EORTC GCG. *J Clin Oncol.* 2006;24:4699-4707.

4. Markman M, Webster K, Zanotti K, Kulp B, Peterson G, Belinson J. Phase 2 trial of single-agent gemcitabine in platinum-paclitaxel refractory ovarian cancer. *Gynecol Oncol.* 2003;90:593-596.

5. Ponnusamy MP, Venkatraman G, Singh AP, et al. Expression of TAG-72 in ovarian cancer and its correlation with tumor stage and patient prognosis. *Cancer Lett.* 2007;251:247-257.

6. Johnson VG, Schlom J, Paterson AJ, Bennett J, Magnani JL, Colcher D. Analysis of a human tumor-associated glycoprotein (TAG-72) identified by monoclonal antibody B72.3. *Cancer Res.* 1986;46:850-857.

7. Thor A, Szpak CA, Gorstein F, Schlom J, Ohuchi N, Johnston WW. Tumor-Associated Glycoprotein (TAG-72) in Ovarian Carcinomas Defined by Monoclonal Antibody 872.3. *J of Natl Cancer I.* 1986;76:995-1006.

8. Osteen KG, Anderson TL, Schwartz K, Hargrove JT, Gorstein F. Distribution of tumor-associated glycoprotein-72 (TAG-72) expression throughout the normal female reproductive tract. *Int J Gynecol Pathol.* 1992;11:216-220.

9. Muraro R, Kuroki M, Wunderlich D, et al. Generation and characterization of B72.3 second generation monoclonal antibodies reactive with the tumor-associated glycoprotein 72 antigen. *Cancer Res.* 1988;48:4588-4596.

10. Bohdiewicz PJ, Scott GC, Juni JE, et al. Indium-111 OncoScint CR/OV and F-18 FDG in colorectal and ovarian carcinoma recurrences. Early observations. *Clin Nucl Med.* 1995;20:230-236.

11. DeNardo SJ, DeNardo GL. Targeted radionuclide therapy for solid tumors: An overview. *International Journal of Radiation Oncology*Biology*Physics.* 2006;66:S89-S95.

12. Murray JL, Macey DJ, Kasi LP, et al. Phase II radioimmunotherapy trial with 131I-CC49 in colorectal cancer. *Cancer.* 1994;73:1057-1066.

13. Alvarez RD, Partridge EE, Khazaeli MB, et al. Intraperitoneal Radioimmunotherapy of Ovarian Cancer with177Lu-CC49: A Phase I/II Study. *Gynecologic Oncology.* 1997;65:94-101.

14. Alvarez RD, Huh WK, Khazaeli MB, et al. A Phase I study of combined modality (90)Yttrium-CC49 intraperitoneal radioimmunotherapy for ovarian cancer. *Clin Cancer Res.* 2002;8:2806-2811.

15. Larson SM, Carrasquillo JA, Cheung N-KV, Press OW. Radioimmunotherapy of human tumours. *Nature reviews Cancer.* 2015;15:347-360.

16. Sgouros G, Roeske JC, McDevitt MR, et al. MIRD Pamphlet No. 22 (abridged): radiobiology and dosimetry of alpha-particle emitters for targeted radionuclide therapy. *J Nucl Med.* 2010;51:311-328.

17. Cherel M, Gouard S, Gaschet J, et al. 213Bi radioimmunotherapy with an anti-mCD138 monoclonal antibody in a murine model of multiple myeloma. *J Nucl Med.* 2013;54:1597-1604.

18. Orozco JJ, Back T, Kenoyer A, et al. Anti-CD45 radioimmunotherapy using (211)At with bone marrow transplantation prolongs survival in a disseminated murine leukemia model. *Blood.* 2013;121:3759-3767.

19. Behling K, Maguire WF, Lopez Puebla JC, et al. Vascular Targeted Radioimmunotherapy for the Treatment of Glioblastoma. *J Nucl Med.* 2016;57:1576-1582.

20. Juergens RA, Zukotynski KA, Juneau D, et al. A phase I study of [225Ac]-FPI-1434 radioimmunotherapy in patients with IGF-1R expressing solid tumors. *Journal of Clinical Oncology.* 2019;37:TPS3152-TPS3152.

21. Scheinberg DA, McDevitt MR. Actinium-225 in targeted alpha-particle therapeutic applications. *Curr Radiopharm.* 2011;4:306-320.

22. Borchardt PE, Yuan RR, Miederer M, McDevitt MR, Scheinberg DA. Targeted actinium-225 in vivo generators for therapy of ovarian cancer. *Cancer Res.* 2003;63:5084-5090.

23. Kennel SJ, Brechbiel MW, Milenic DE, Schlom J, Mirzadeh S. Actinium-225 conjugates of MAb CC49 and humanized delta CH2CC49. *Cancer Biother Radiopharm.* 2002;17:219-231.

24. Miederer M, McDevitt MR, Borchardt P, et al. Treatment of neuroblastoma meningeal carcinomatosis with intrathecal application of alpha-emitting atomic nanogenerators targeting disialo-ganglioside GD2. *Clin Cancer Res.* 2004;10:6985-6992.

25. Song H, Hobbs RF, Vajravelu R, et al. Radioimmunotherapy of breast cancer metastases with alpha-particle emitter 225Ac: comparing efficacy with 213Bi and 90Y. *Cancer Res.* 2009;69:8941-8948.

26. Li L, Bading J, Yazaki PJ, et al. A versatile bifunctional chelate for radiolabeling humanized anti-CEA antibody with In-111 and Cu-64 at either thiol or amino groups: PET imaging of CEA-positive tumors with whole antibodies. *Bioconjug Chem.* 2008;19:89-96.

27. Bombardieri E, Giammarile F, Aktolun C, et al. 131I/123I-metaiodobenzylguanidine (mIBG) scintigraphy: procedure guidelines for tumour imaging. *Eur J Nucl Med Mol Imaging.* 2010;37:2436-2446.

28. Seki T, Fang J, Maeda H. Enhanced delivery of macromolecular antitumor drugs to tumors by nitroglycerin application. *Cancer Sci.* 2009;100:2426-2430.

29. Schwartz J, Jaggi JS, O'Donoghue JA, et al. Renal uptake of bismuth-213 and its contribution to kidney radiation dose following administration of actinium-225-labeled antibody. *Phys Med Biol.* 2011;56:721-733.

30. Song EY, Qu CF, Rizvi SM, et al. Bismuth-213 radioimmunotherapy with C595 anti-MUC1 monoclonal antibody in an ovarian cancer ascites model. *Cancer Biol Ther.* 2008;7:76-80.

31. Fujimori K, Covell DG, Fletcher JE, Weinstein JN. A modeling analysis of monoclonal antibody percolation through tumors: a binding-site barrier. *J Nucl Med.* 1990;31:1191-1198.

32. Azzi S, Hebda JK, Gavard J. Vascular permeability and drug delivery in cancers. *Front Oncol.* 2013;3:211.

33. Suliman G, Pomme S, Marouli M, et al. Half-lives of 221Fr, 217At, 213Bi, 213Po and 209Pb from the 225Ac decay series. *Appl Radiat Isot.* 2013;77:32-37.

34. Vallabhajosula S, Smith-Jones PM, Navarro V, Goldsmith SJ, Bander NH. Radioimmunotherapy of prostate cancer in human xenografts using monoclonal antibodies specific to prostate specific membrane antigen (PSMA): studies in nude mice. *Prostate.* 2004;58:145-155.

Table 1: Mean Survival and Total Absorbed Tumor Dose for ^{225}Ac Radioimmunotherapy of OVCAR3 Xenografts.

	Control[1] n=16	7.4 kBq untargeted antibody n=6	1.85 kBq huCC49 n=6	3.7 kBq huCC49 n=6	7.4 kBq huCC49 n=6	Multi-tx untargeted antibody n=8	Multi-tx huCC49 n=8
Mean survival	32.3	87.9*	54.6*	81.6*	103*	37.6[ns]	86.0
Max tumor dose (Gray)[2]	n/a	2.93	2.50	5.01	10.0	7.74	17.7
Min tumor dose (Gray)[3]	n/a	0.73	0.63	1.25	2.50	1.94	4.43

[1] Number of radioimmunotherapy controls combined from single and multi-treatment groups.

[2] Max dose: assumed delivery of all four α-particles at site of tumor based on biodistribution study.

[3] Min dose: assume delivery of only one α-particle at site of tumor based on biodistribution study.

* Significant difference compared to no RIT controls.

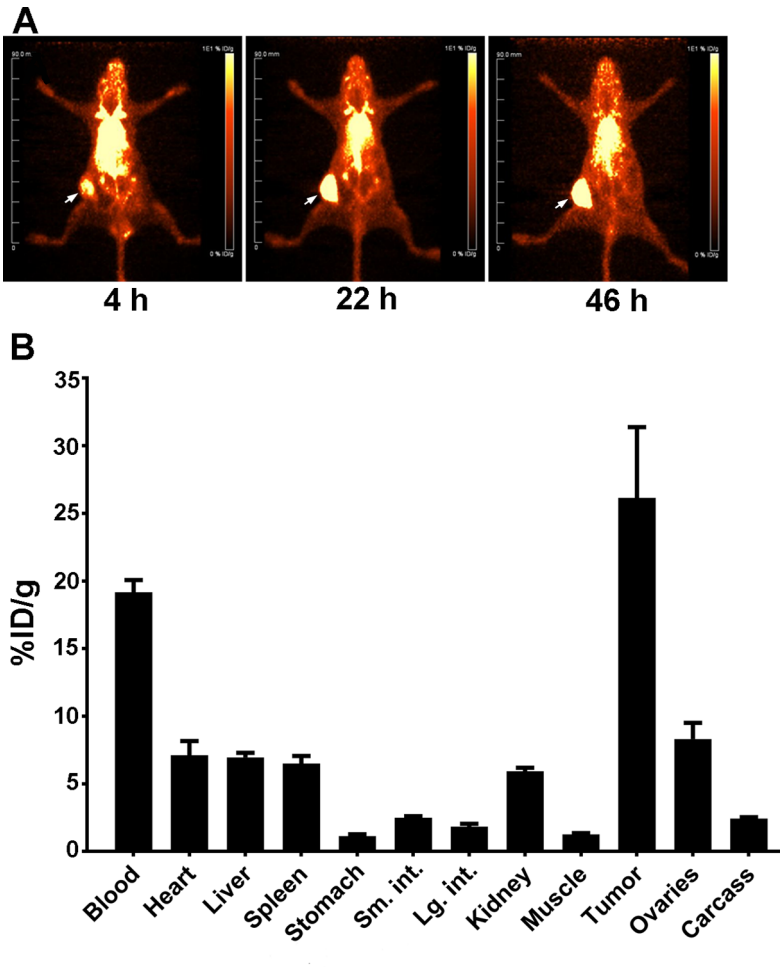

Figure 1. PET Imaging of ^{64}Cu-DOTAylated- huCC49 mice bearing OVCAR3 xenografts. A. PET images of ^{64}Cu-DOTAylated-huCC49 (Arrow indicates tumor site). B. Biodistribution at terminal time point (n=4). Total dose to tumor was 7.8% (26 %ID/g x 0.30 g= 7.8% ID).

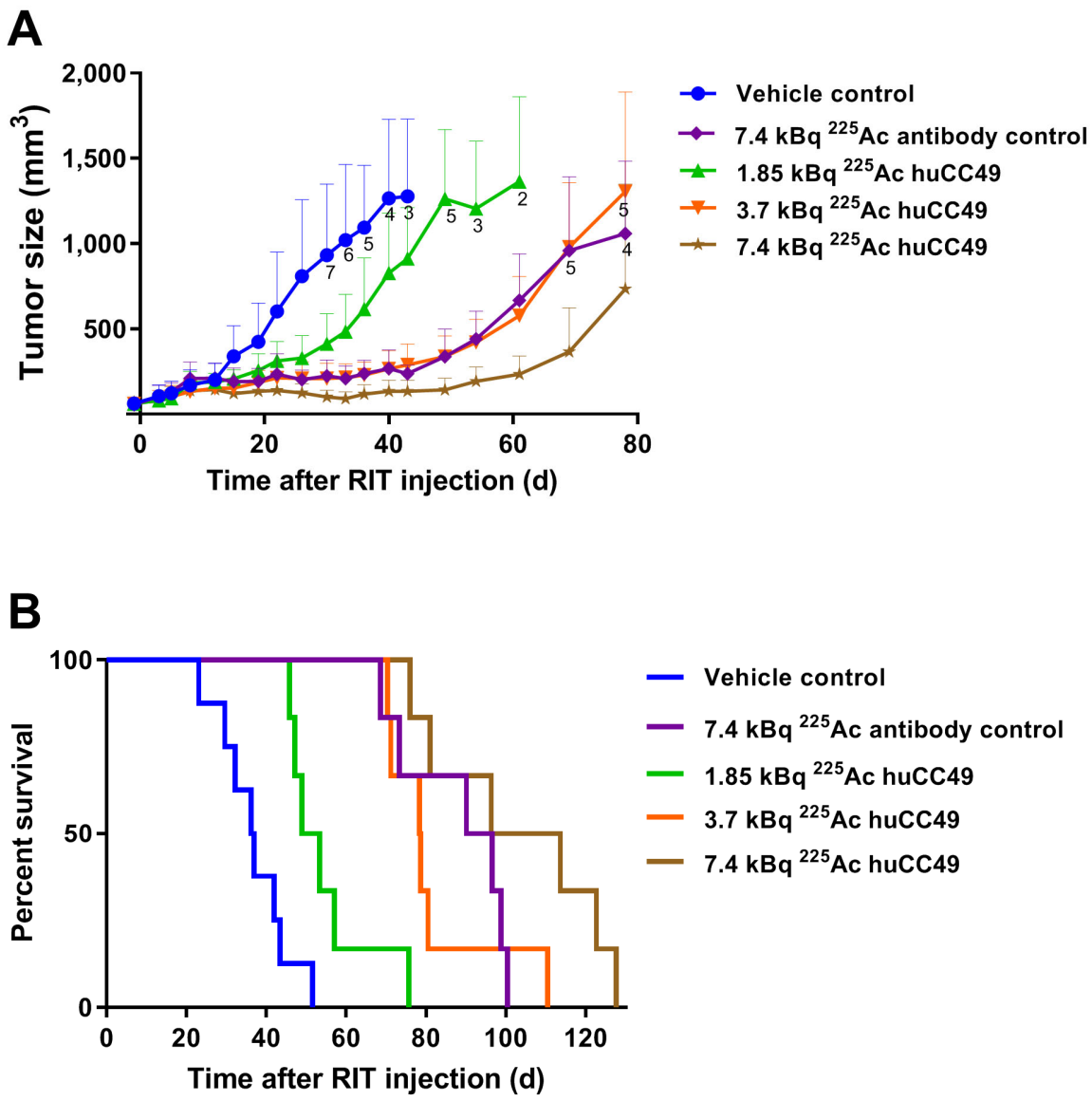

Figure 2. Dose escalation of ^{225}Ac-DOTAylated- huCC49 mice bearing OVCAR3 xenografts. A. Tumor volume vs time post RIT. B. Kaplan-Meier survival plot (n=8 for control group, n=6 for all other groups). Tumor growth curves of the 7.4 kBq untargeted (***, p=0.0001), 3.7 kBq targeted (***, p=0.0001) and the 7.4 kBq targeted (***, p=<0.0001) groups were statistically significant compared to the untreated controls. Survival curves of the 7.4 kBq untargeted (**, p=0.0011), 1.85 kBq targeted (**, p=0.0054), 3.7 kBq targeted (***, p=0.0003), and 7.4 kBq targeted (***, p=0.0003) groups were statistically significant compared to controls.

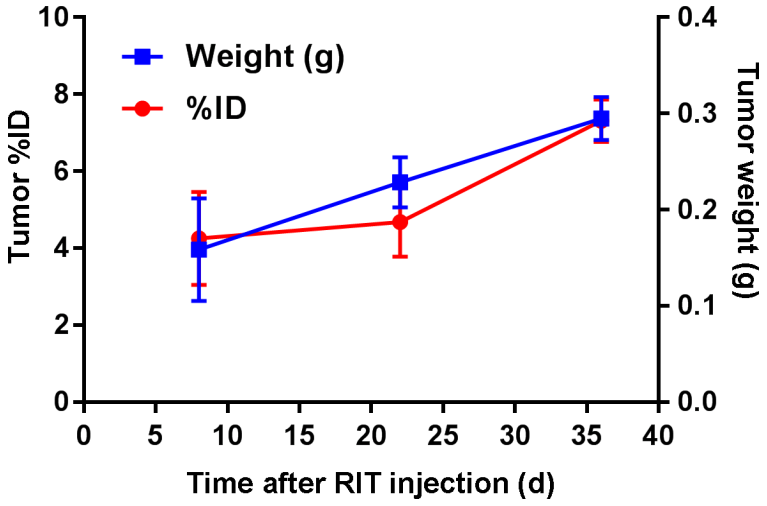

Figure 3. TAG-72 expression measured by ^{64}Cu-DOTAylated-huCC49 tumor uptake following a single dose of 3.7 kBq of ^{225}Ac-DOTAylated-huCC49. Two mice, per week, at 1, 3, and 5 weeks post RIT (3.7 kBq) were injected with ^{64}Cu-DOTAylated-huCC49, and tumor uptake and weight measured 72hr post injection.

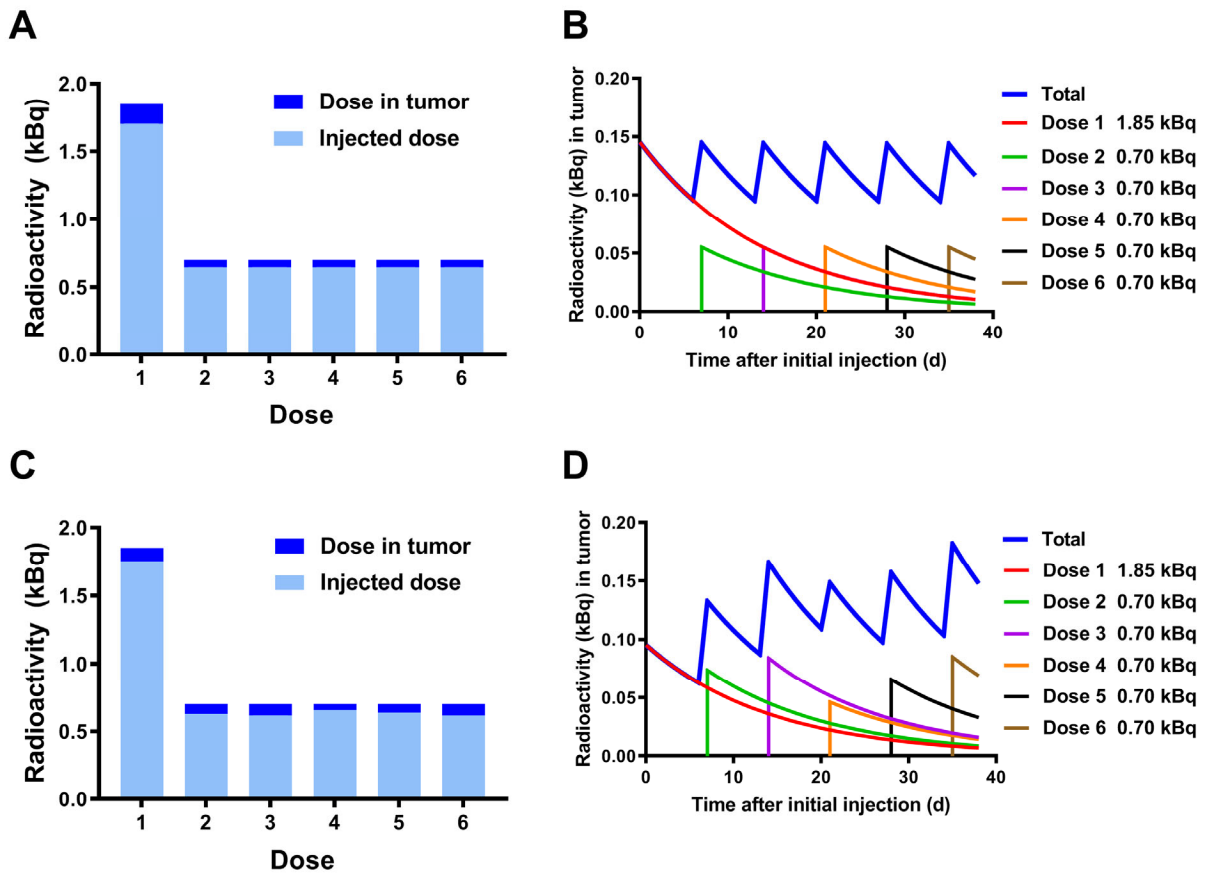

Figure 4. Theoretical and actual doses administered in the multi-treatment strategy. A. The total calculated dose in kBq given compared to the amount found in tumor with initial dose of 1.85 kBq followed by 5 subsequent doses of 0.70 kBq (see Figure 1). B. Total calculated amount of radioactivity in the tumor accounting for radioactive decay. C. The actual injected dose in kBq determined by an ^{111}In-DOTAylated-huCC49 biodistribution performed after each dose of ^{225}Ac-DOTAylated-huCC49 compared to the amount in the tumor where the initial dose is 1.85 kBq followed by 5 subsequent doses of 0.70 kBq. D. Total actual amount of radioactivity in the tumor accounting for radioactive decay.

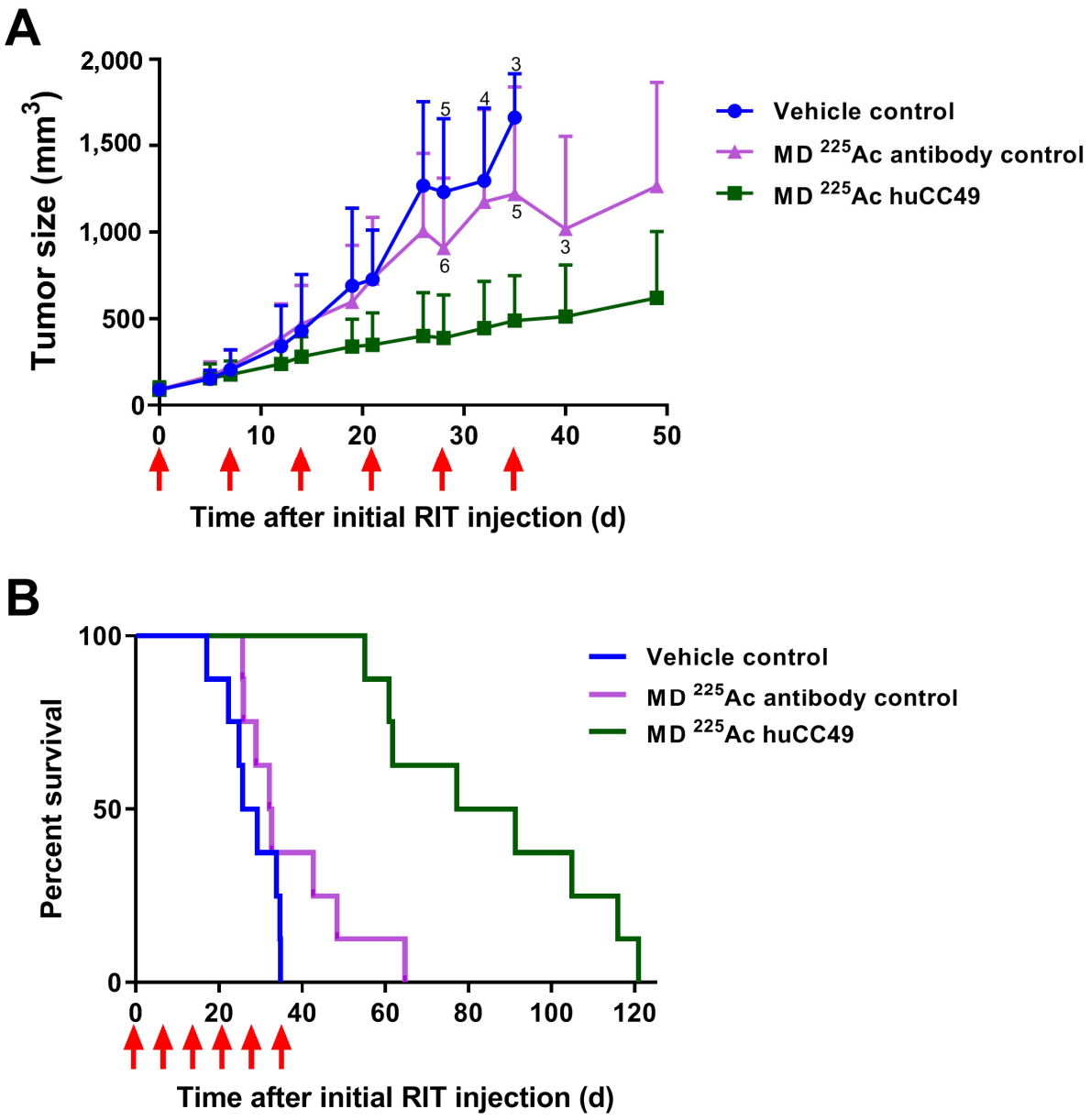

Figure 5. Multi-treatment RIT mice bearing OVCAR3 xenografts. Doses were given at days 0, 7, 14, 21, 28, and 35. A. Tumor volume vs time post RIT. B. Kaplan-Meier survival plots (n=8 for all groups). Tumor growth curve of the RIT targeted group was statistically significant (*, p=0.043) compared to controls. The survival curve of the targeted RIT was statistically significant (***, p=<0.0001) compared to controls.

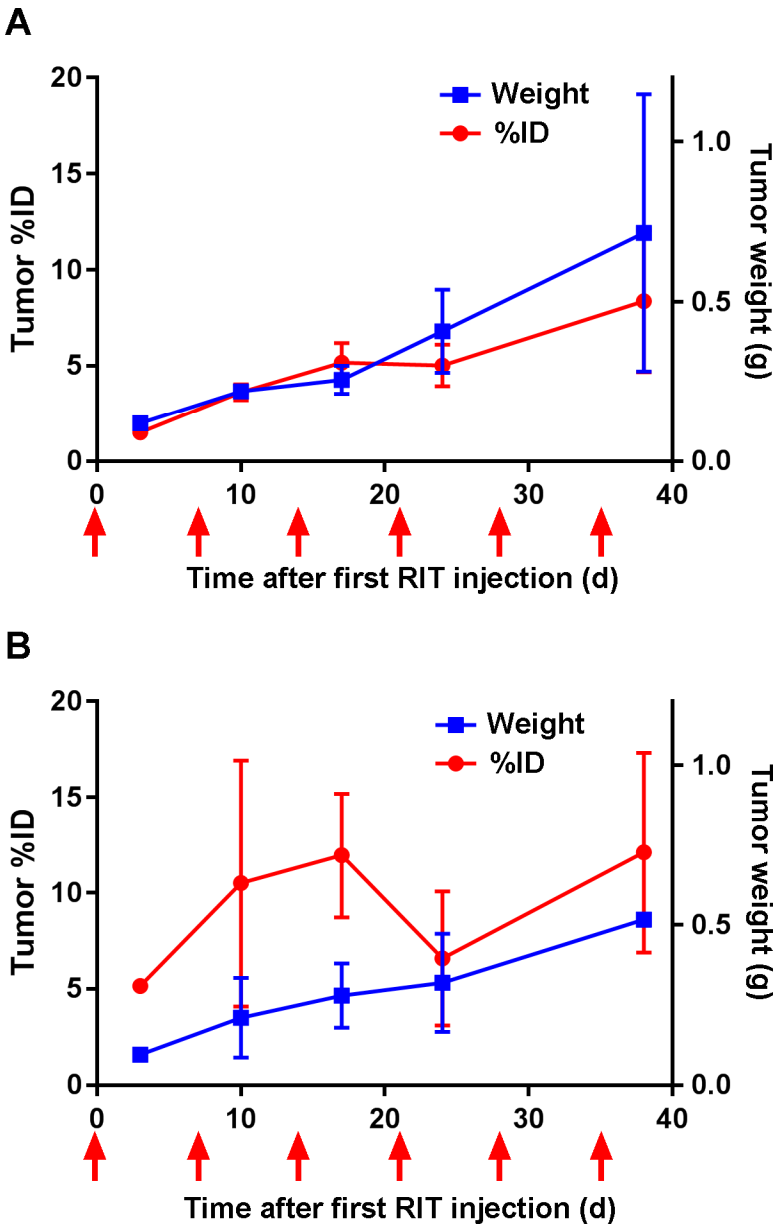

Figure 6. Antibody uptake and tumor weights in targeted and untargeted RIT. Two mice at indicated time points post RIT were injected with either ^{111}In-labeled untargeted (A) or ^{111}In-labeled targeted (B) antibodies in place of each RIT dose. Timing of ^{111}In- labeled antibody injections are indicated with red arrows.

TAG-72 targeted alpha-radionuclide therapy of ovarian cancer using actinium-225 labeled DOTA-huCC49 antibody

Megan Minnix [1,2], Lin Li [1], Paul J. Yazaki [1], Aaron D. Miller[1], Junie Chea [3], Erasmus Poku [3], Russell C. Rockne[4], David Colcher [1] and John E. Shively [1,*]

Supplementary Material

MATERIALS AND METHODS

Humanization of anti-TAG72 huCC49 antibody. The humanized variable domains of the anti-TAG72 huCC49 delta CH2 mAb was obtained from the literature (1). The amino acid sequence (1 letter code) of the immunoglobulin variable domains are listed:

Variable light domain:
DIVMSQSPDSLAVSLGERVTLNCKSSQSLLYSGNQKNYLAWYQQKPGQSPKLLIYWAS
ARESGVPDRFSGSGSGTDFTLTISSVQAEDVAVYYCQQYYSYPLTFGAGTKLELKRTV
AAPSVFIFPPSDEQLKSGTASVVCLLNNFYPREAKVQWKVDNALQSGNSQESVTEQDS
KDSTYSLSSTLTLSKADYEKHKVYACEVTHQGLSSPVTKSFNRGEC

Variable heavy domain:

QVQLVQSGAEVVKPGASVKISCKASGYTFTDHAIHWVKQNPGQRLEWIGYFSP
GNDDFKYNERFKGKATLTADTSASTAYVELSSLRSEDTAVYFCTRSLNMAYWGQGTLV
TVSSASTKGPSVFPLAPSSKSTSGGTAALGCLVKDYFPEPVTVSWNSGALTSGVHTFP
AVLQSSGLYSLSSVVTVPSSSLGTQTYICNVNHKPSNTKVDKKV

The genes encoding the huCC49 delta CH2 were reformatted into a full length human IgG1 mAb by cDNA synthesis (GeneArt Gene Synthesis, ThermoFisher). The light and heavy chains were cloned into the dual chain pEE12/6 expression vector (Lonza, Basel, Switzerland). The huCC49 was transiently expressed in EXPI293 cells (Life Technologies) and the 6 day cell culture supernatant was purified by Protein A (Sigma Millipore, Burlington, MA) and ceramic hydroxyapatite (Bio-Rad, Hercules, CA) chromatography. The purified antibody was characterized by SDS-PAGE and size exclusion chromatography using Superdex 200 (GE Healthcare Life Sciences,

Pittsburgh, PA) and showed a purity greater than 98%. Kinetic affinity analysis was conducted by surface plasmon resonance on a Biacore X100 (GE Healthcare). Recombinant TAG-72 antigen (Bio-Rad) was immobilized on a CM-5 chip, and serial concentrations of muCC49 mAb or huCC49 mAb flowed over the chip. The K_D for the muCC49 mAb was 2.5 x 10^{-8} and huCC49 mAb was 2.3 x 10^{-8}.

References

1. Braslawski, G.R. et al., US Patent No. 7,319,139, Jan 15, 2008.

Absorbed Dose calculations.

Absorbed Dose calculations.

The alpha-particle energy of a single nucleus ^{225}Ac in 1 disintegration was calculated as 27.65 MeV, which accounts for over 90% of the energy released [28]. Using the high LET 27.65 MeV energy per disintegration, the joules released in 1 day from 1 kBq of ^{225}Ac is 3.8 x10^{-4} J. With a half-life of 10 days, the decay-corrected energy released over 38 days is E_{kBq} = 5.12 x10^{-3} J per kBq. The average weight measured from a biodistribution study done in parallel with the therapy studies was used to calculate absorbed dose in Gray (Gy). For the single dose study, the biodistribution group was given 1 dose of 3.7 kBq and 2 mice from this group were euthanized per time point, and the tumor weight was measured. For the multi-dose study, the biodistribution group was given multiple doses of either ^{225}Ac-huCC49 or ^{225}Ac-untargeted control antibody and 2 mice from each group were euthanized per time point, at which point the tumor weights were measured. Because not all of the injected dose reaches the tumor, to calculate the amount of energy (*E'*) released in the tumor, the percent of injected dose measured in the tumor is used to adjust the dose-specific energy:

$$E' = \sum_{\mathrm{i}=1}^{\mathrm{N}} \int_{\mathrm{t_i}}^{\mathrm{t_f}} \alpha_{\mathrm{i}} E_{kBq}\, \mathrm{e}^{-\left(\frac{\ln 2}{\mathrm{t}_{1/2}}\right)\mathrm{t}}\, \mathrm{dt}$$

where the injected dose measured in the tumor after dose *i* (α_i), is given by the biodistribution studies done for both huCC49 and the untargeted control antibody. The injected dose in the tumor after each dose in the multi-therapy treatment was determined by the ^{111}In biodistribution study (**Figure 4C**). The total injected dose is the sum of the individual doses $D = \sum_{i=1}^{N} D^i$ (Single dose: 1.85 kBq, 3.7 kBq, or 7.4 kBq; Multi-treatment: 1.85 kBq (x1) + 0.70 kBq (x5)). The percent of the injected dose in the tumor after a single dose of ^{225}Ac-huCC49 was D^1=5.15%. For dose 5, in the multi-treatment therapy, the injected dose was extrapolated based on slope of the line of the surrounding data points (α_i=.394t-2.86 α_5 = 0.0935), as no biodistribution was done for that time point.

Calculation of tumor growth rate and survival for 5.4 kBq single dose.

Note: This calculation was added in response to review.

Because several factors contribute to overall survival, including tumor burden, treatment toxicity, and inter-individual biological variability, we consider an analysis of tumor growth rates, which is much more consistent across mice and treatment conditions.

We begin by transforming the tumor volume data into the radius of a sphere with an equivalent volume with the formula:

$$r = \left(\frac{3V}{4\pi}\right)^{1/3}$$

For all calculations, we use the average tumor volume across all mice for each time point and treatment condition.

Multiple groups and mathematical models have shown that the radius of untreated tumor growth can grow linearly over time. We can see this in our data for the untreated control arms in both the single and multi-dose experiments. Linear regression of the tumor radius over time has a correlation coefficient of $r > 0.99$. The multi-dose controls have been scaled to have the same initial tumor radius as the single dose controls (**Supplemental Figure S8**).

Now that we have established that in our model, tumor radius grows linearly over time if untreated, we introduce the concept of a fatal (or maximal) tumor burden (FTB). In order to compare across all conditions and dose levels, the FTB is defined as the greatest lower bound of tumor radius over all the single dose experiments, and is approximately FTB = 5.6mm. Because the therapeutic effect of RIT fades over time as the radionuclide decays and the targeted tumor cells are killed, the treatment eventually fails and the tumor returns to a linear radial growth pattern. This can be seen in the single dose experiment by performing linear regression (black lines) on the last 3 time points for each dose level and control. This linear regression is used to calculate the precise time the FTB is attained, indicated with a * on the graph (**Supplemental Figure S9**).

Now we compare the multi-dose (5.4 kBq = 1.85+0.70 x5 kBq) experiment with the single dose experiments to address the concern that there was not a 5.4 kBq single dose control. So let's look at the growth curve of the multi-dose experiment in comparison to the 3.7 kBq and 7.4 kBq single dose data. We scale the tumor radius of the multi-dose data so that the initial sizes are equal to the 3.7 kBq single dose.

Using the same approach as before, by fitting a line to the last 3 data points in the multi-dose experiment, we extrapolate the growth curve to predict a time of FTB, which falls between the 3.7 kBq and 7.4 kBq single doses. This gives a predicted time to FTB of T = 71.8 days. Although the multi-dose tumor radius is consistently larger than the single 3.7 kBq or 7.4 kBq doses, the growth rate overall is significantly reduced.

If we want to predict what would be the result of a 5.4 kBq single dose treatment, we plot the time to FTB versus dose. This plot shows the time to FTB versus Dose for the single dose experiments (**Supplemental Figure S10**).

First, we tried a linear fit to this data, but it didn't look right, and it predicted that more dose would result in longer time to FTB indefinitely, which is clearly not correct. Since we have 4 data points (control (Dose=0) + 3 dose levels) we have enough data to fit a quadratic function. This predicts the time to FTB for a single 5.4 kBq dose, and also makes an interesting prediction that approximately 9.25 kBq is an optimal dose—in the sense of delaying the time to FTB, not necessarily survival. Beyond that, say 14.8 kBq, we would not predict a benefit in reducing or delaying tumor growth, for example, due to toxicity or very rapid treatment effect resulting in earlier, more rapid tumor re-growth.

The time to FTB for the multi-dose experiment predicted by extrapolating the growth curve is:

T = 71.8 days.

The predicted time to FTB given by the quadratic fit to the single-dose data above is:

T = 71.1 days.

One final question: How do the tumor growth rates compare?

The 5.4 kBq multi-dose has a greatly reduced overall tumor growth rate as compared to the controls and 1.85, 3.7, 7.4 kBq single dose treatments (**Supplemental Figure S11**).

What this means is:

We don't have to do a 5.4 kBq single dose experiment, because

1) we can predict what would happen. This is because the overall survival and tumor growth curves are well separated from each other, so we have confidence in interpolating between the dose levels. In other words, 5.4 kBq will be better than 3.7 kBq, but not as good as 7.4 k Bq, both in terms of survival and in terms of tumor growth.

2) Interestingly, what we predict is that although a single 5.4 kBq dose would have almost exactly the same effect on the time to FTB, our multi-dose experiment has two distinct advantages:
    a. Less toxicity
    b. Greatly reduced overall tumor growth rate
    c. It also has the *potential to mitigate therapeutic resistance

Supplemental Figure S1. TAG-72 expression of OVCAR3 xenografts in NSG mice.

NSG mice with s.c. OVCAR3 xenografts were harvested about 60-90 days post injection and stained with human anti-TAG-72 antibody, huCC49 (**A**) and (**B**) or a control anti-CD38 antibody (**C**) and (**D**).

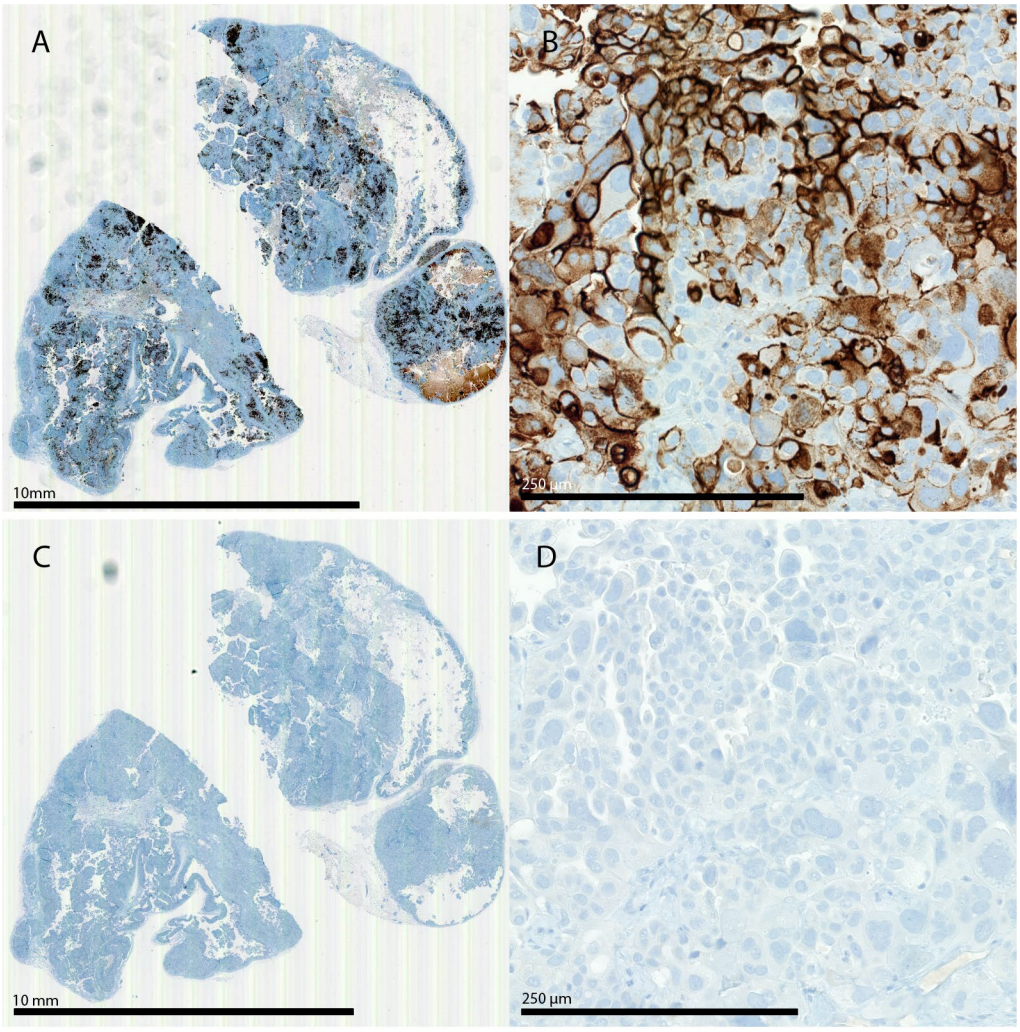

Supplemental Figure S2. Characterization of DOTAylated-huCC49. Q-TOF-MS analysis of huCC49 before and after DOTAylation. **A.** Light chain before (upper) and after (lower) DOTAylation**. B.** Heavy chain before (upper) and after (lower) DOTAylation. The average number of DOTA/Ab was calculated as 3.0 from this analysis. Elution of I-124 labeled huCC49 on SEC before (**C**) and after (**D**) addition of 20-fold excess of bovine submaxillary mucin. ITLC of ^{225}Ac-DOTAylated-huCC49 showed >95% incorporation with 10 mM DTPA chase (data not shown).

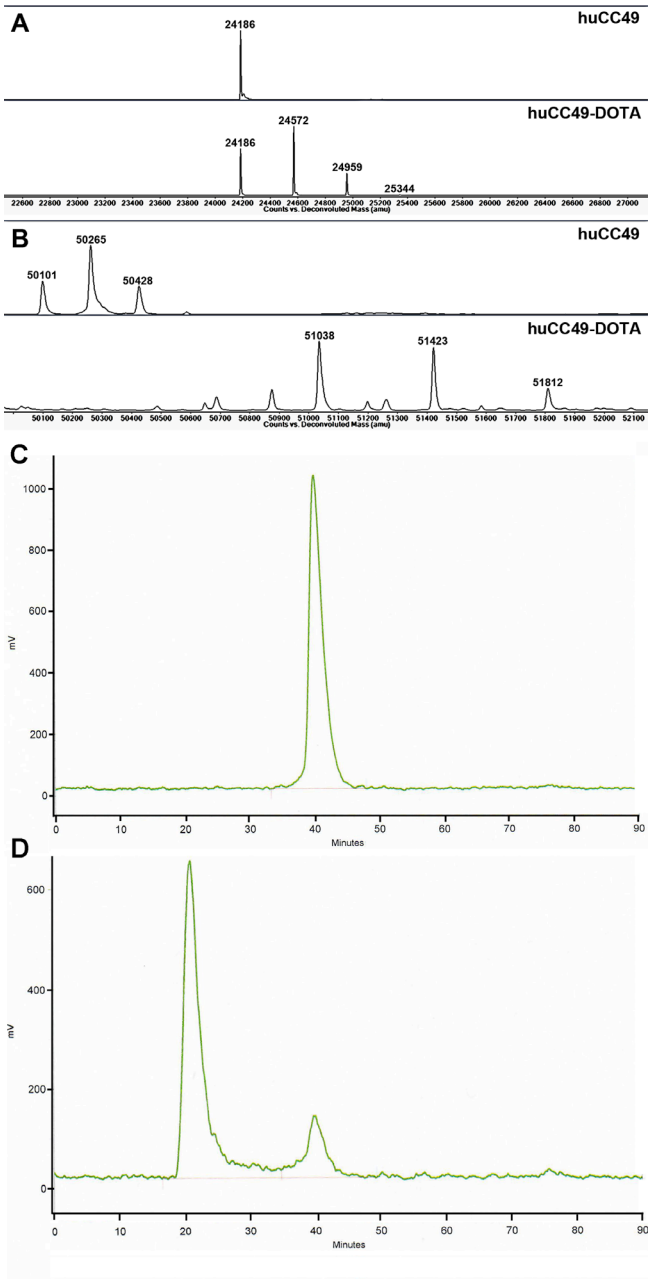

Supplemental Figure S3. Blood Clearance of murine CC49 and humanized CC49. Kinetics of ^{124}I labeled murine or humanized CC49 (370 kBq/mouse) in OVCAR3 xenografted female NSG mice. The average counts in blood are shown in graph (n=2/time point).

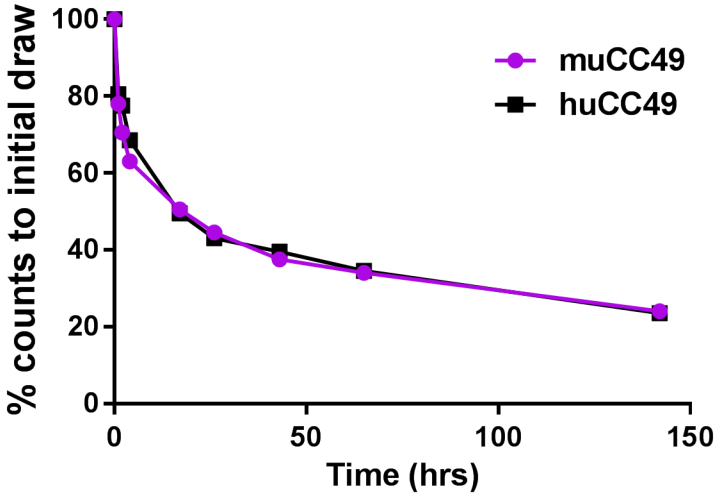

Supplemental Figure S4. Single dose therapy with ^{225}Ac-DOTAylated-huCC49 in OVCAR3 xenografts in female NSG mice. Red arrow indicates day RIT given. Graphs are of individual mice within each treatment group.

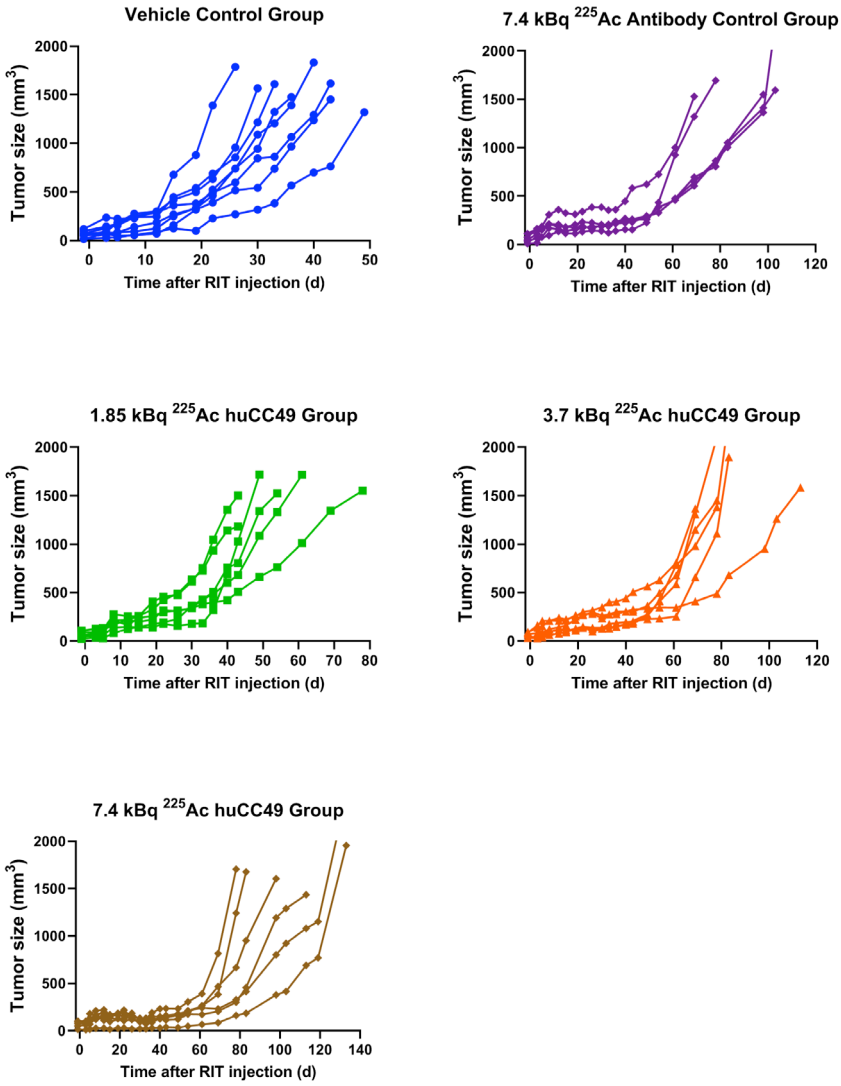

Supplemental Figure S5. Whole body toxicity of single dose RIT in OVCAR3 xenografts in female NSG mice. Toxicity, as measured by weight loss, of the single dose RIT treated groups (n=8 for control group, n=6 for all other groups). The whole body toxicity curves of the 7.4 kBq ^{225}Ac untargeted antibody control (****, p=<0.0001), 1.85 kBq ^{225}Ac huCC49 (**, p=0.0067), 3.7 kBq ^{225}Ac huCC49 (***, p=0.0001), and 7.4 kBq ^{225}Ac-huCC49 (****, p=<0.0001) groups were statistically significant compared to the vehicle control. Statistics were carried out using one-way ANOVA, up to day 43.

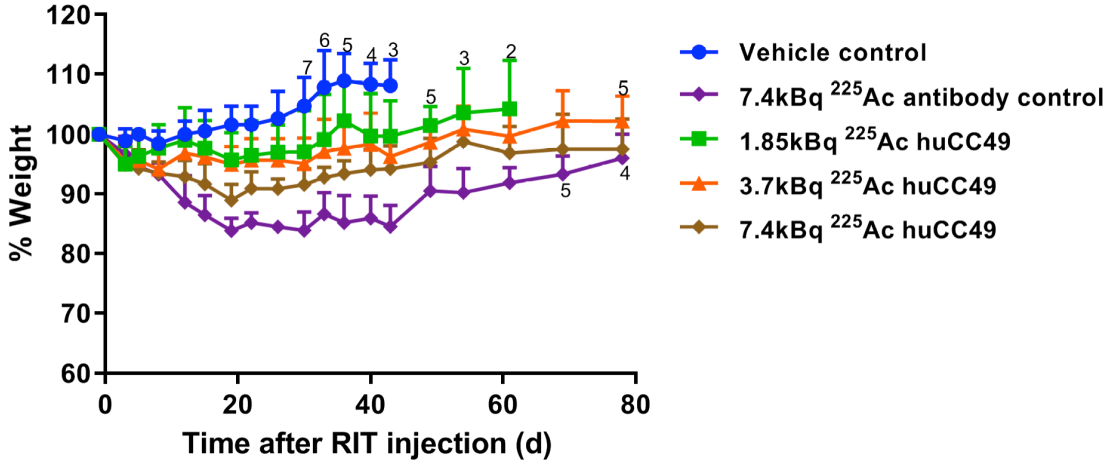

Supplemental Figure S6. Multi-dose therapy ^{225}Ac-DOTAylated-huCC49 in OVCAR3 xenografts in female NSG mice. Doses were given at day 0, day 7, day 14, day 21, day 28, and day 35. Graphs are of individual mice within each treatment group (n=8 for all groups).

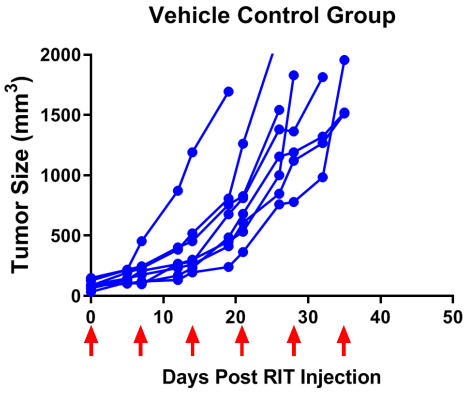

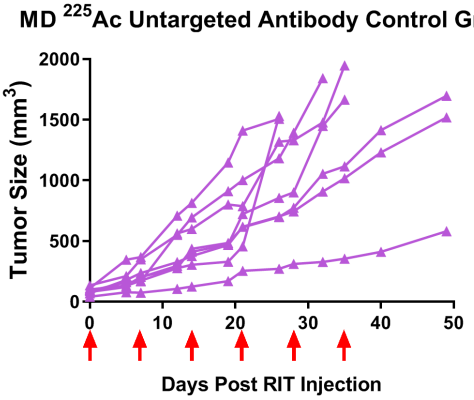

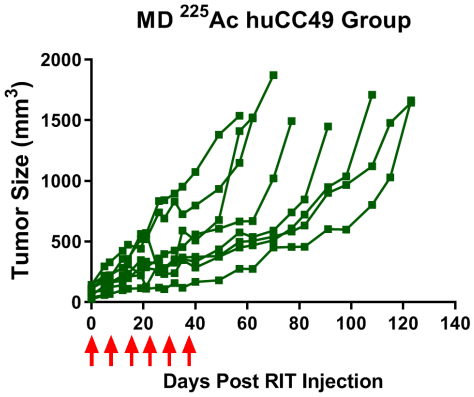

Supplemental Figure S7. Whole body toxicity of multi-dose RIT in OVCAR3 xenografts in female NSG mice. Toxicity, as measured by weight loss, of the multi-dose RIT treated groups (n=8 for all groups). The whole body toxicity curve of the MD ^{225}Ac untargeted antibody control group (***, p=0.0009) was statistically significant compared to the vehicle control. Statistics were carried out using one-way ANOVA, up to day 35.

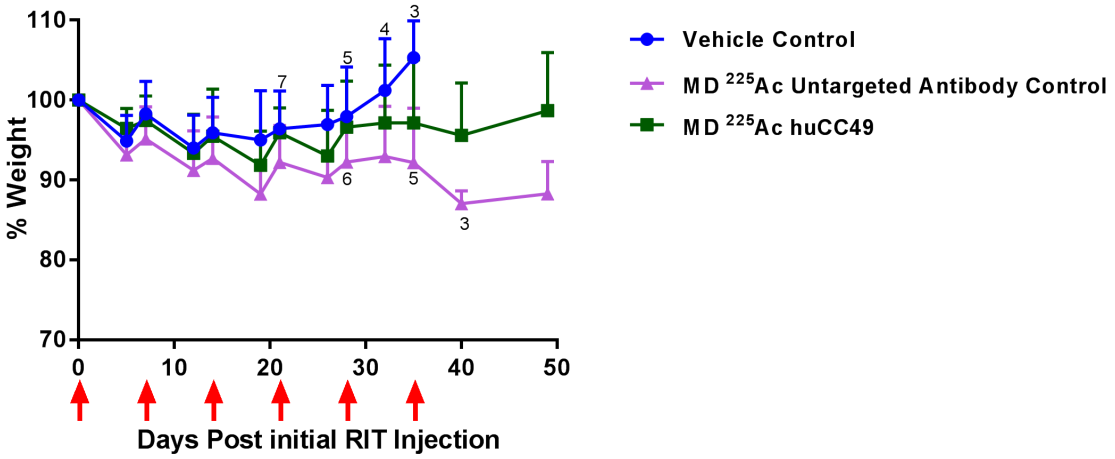

Supplemental Figure S8. Calculated average tumor volume across all mice for each time point and treatment condition. There is a linear correlation of tumor radius with time of treatment.

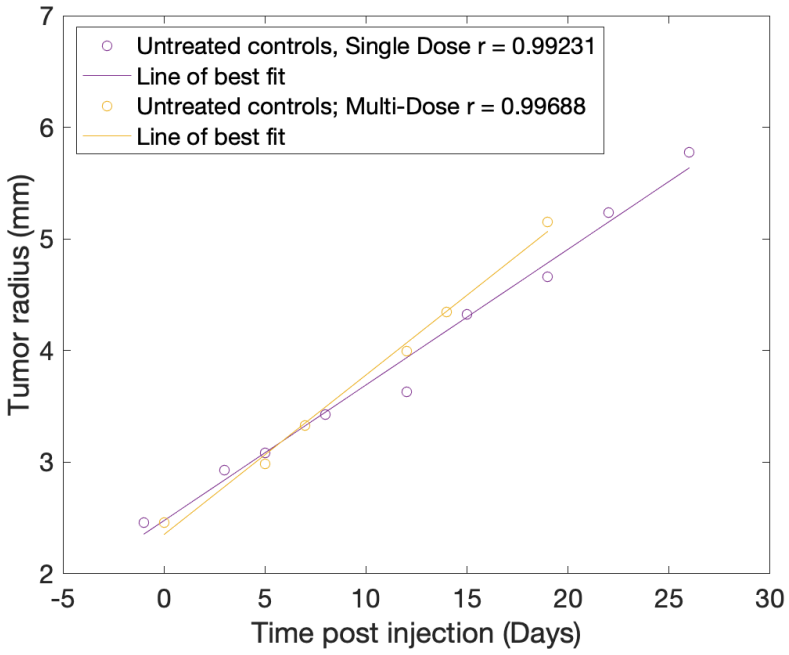

Supplemental Figure S9. A linear regression analysis to calculate the precise time the FTB is attained. A. Time to fatal tumor burden (FTB) for single doses. **B**. Time to FTB with multiple dose included.

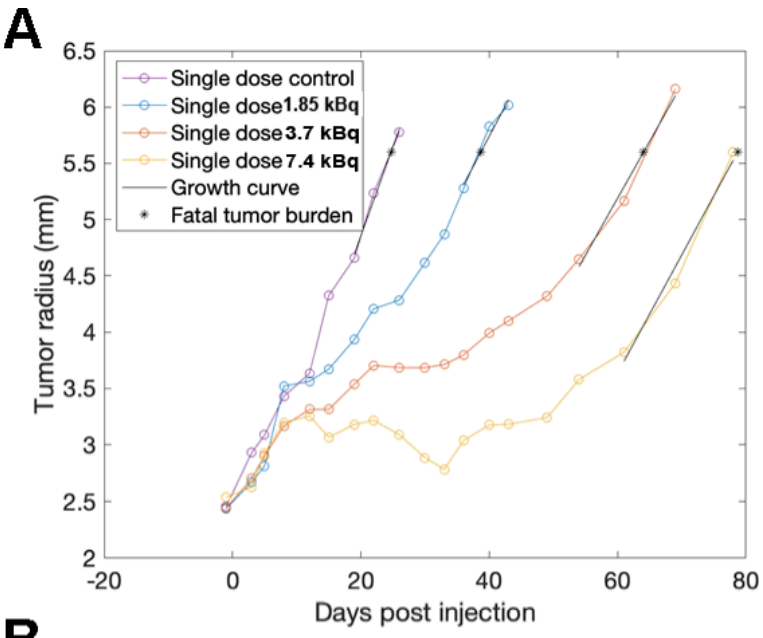

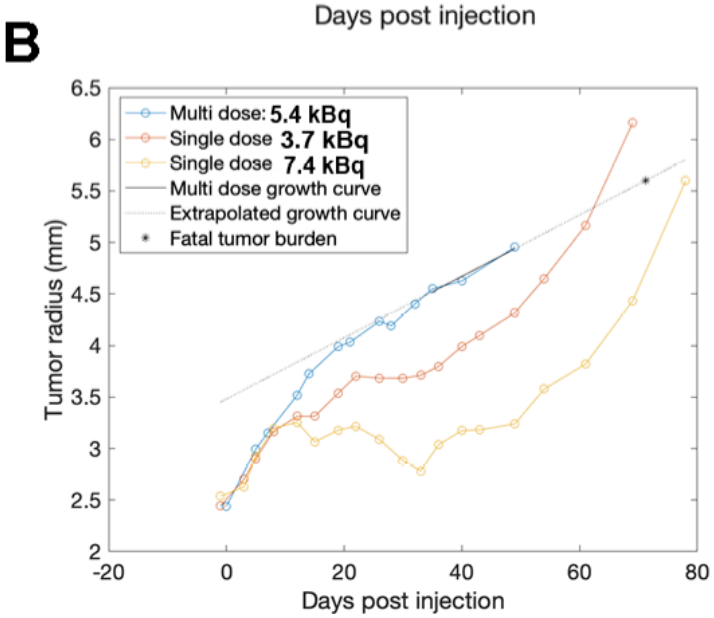

Supplemental Figure S10. Plot of time to FTB versus dose. Data was fitted to a quadratic equation.

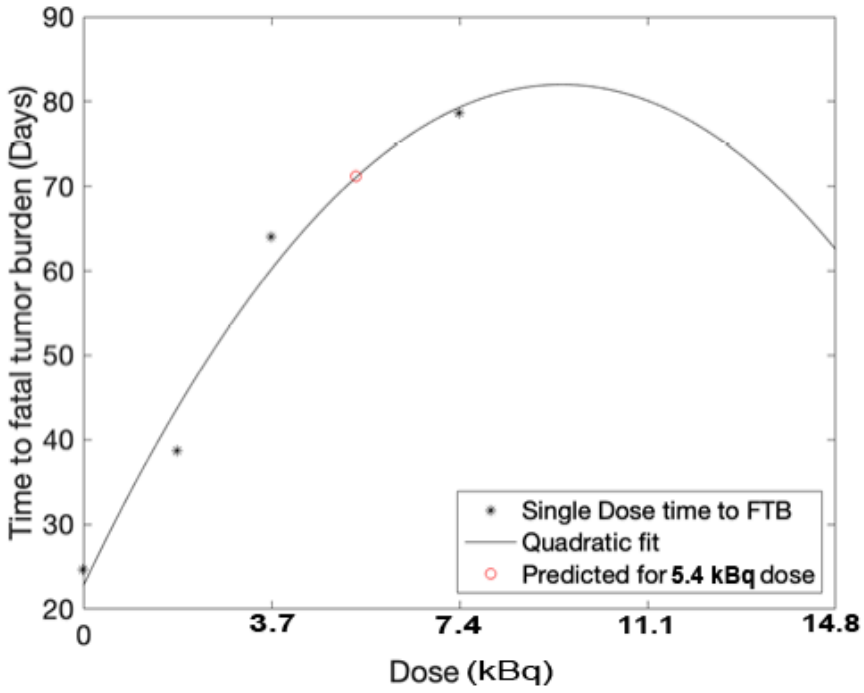

Supplemental Figure S11. Graph of tumor growth rate vs dose. All of the tumor growth rates except for the 5.4 kBq dose are shown for single treatments. The 5.4 kBq growth rate was for the multi-treatment strategy.